Quantification of hydrogen peroxide during the low-temperature oxidation of alkanes.

Chiheb Bahrini[#], Olivier Herbinet[#], Pierre-Alexandre Glaude[#], Coralie Schoemaecker[$], Christa Fittschen[$], Frédérique Battin-Leclerc[#]*.

[#]LRGP, Université de Lorraine, CNRS, ENSIC, BP 20451, 1 rue Grandville, 54001 Nancy, France.

[$]PC2A, University Lille 1, CNRS, Cité Scientifique, Bât. C11, 59655 Villeneuve d'Ascq, France.

Supplementary Information

Table of Content

1. Additional details about the experimental facility

The oxidation of *n*-butane was performed using a spherical quartz jet-stirred reactor. This is an isothermal and isobaric continuous flow reactor working at steady state which is well adapted to kinetic studies. It was designed to obtain homogeneous concentrations and temperature of the gas phase inside the reactor during residence times between 0.5 and 10 s. Species exiting the reactor were analyzed using two different techniques: gas chromatography and cw-CRDS. Figure S1 presents a photography of the reactor connected to the CRDS cell.

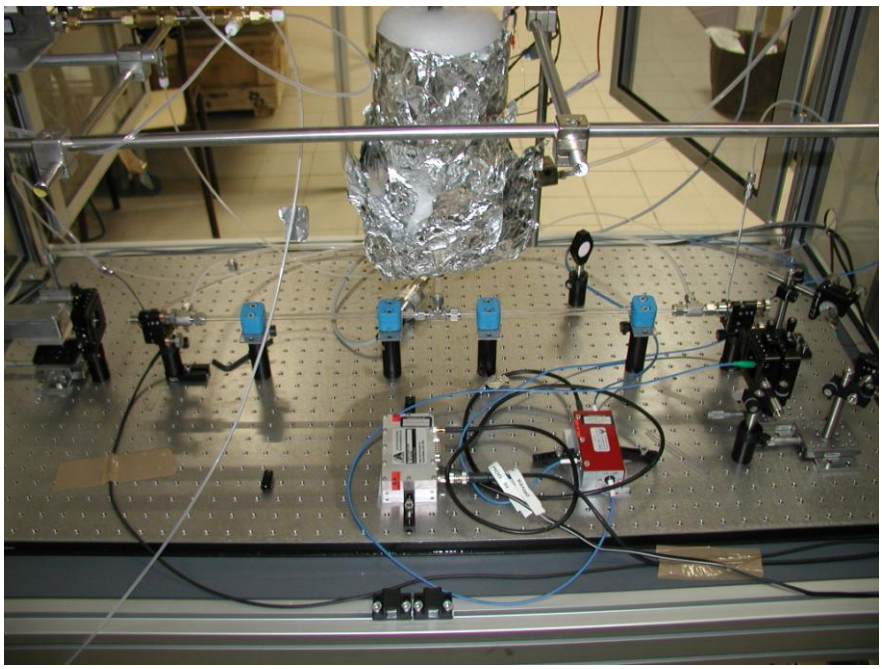

Figure S1. Photography of the used apparatus.

1.1 The jet-stirred reactor

This type of reactor was already used for numerous gas-phase kinetic studies (e.g. [1][2][3]). Figure S2 shows the reactor before the insertion of the sampling cone-like nozzle. It is a spherical reactor in which diluted reactant enters through an injection cross located in its centre. The diameter of the reactor is about 50 mm and its volume is about 85 cm^3. It can be considered as well stirred for a mean residence time (τ) between 0.5 and 6 s (in the latter case, the Reynolds number is 1070 and the recirculation ratio 127)[4]. The stirring of the whole reactor volume is achieved by the mean of four turbulent gas jets directed in different directions and produced by the four nozzles of the injection cross in the centre of the reactor. Inside diameter of the nozzles is about 0.3 mm.

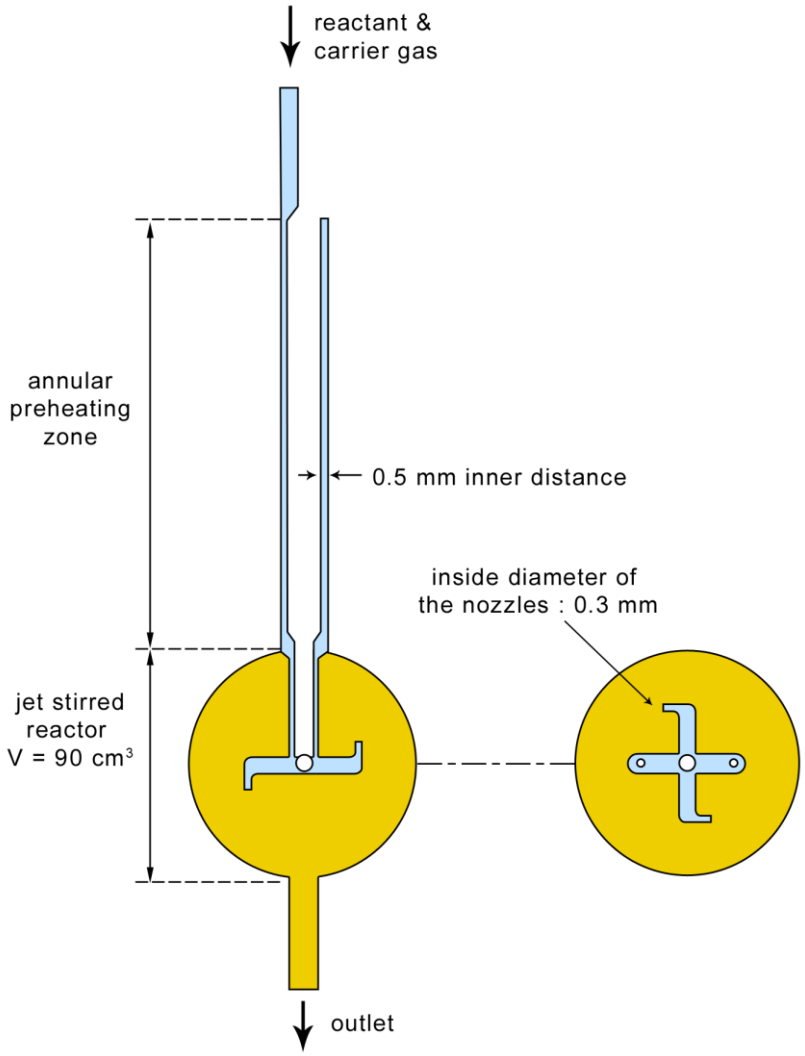

Figure S2. Scheme of the jet-stirred reactor without the sampling probe.

The quartz reactor is preceded by a quartz annular preheating zone in which the temperature of the gases is increased up to the reactor temperature before entering inside. The annular preheater is made of two concentric tubes, the inter-annular distance of which is about 0.5 mm. Gas mixture residence time inside the annular preheater is very short compared to its residence time inside the reactor (about a few percents). Both spherical reactor and annular preheating zone are heated by the mean of "Thermocoax" heating resistances rolled up around their wall. Reaction temperature measurement is made by means of a thermocouple K (provided by Thermocoax, no correction needed) which is located inside the intra-annular space of the preheating zone and the extremity of which is on the level of the injection cross. The dilution was large enough so that a maximum increase of temperature of 5 K was obtained when starting the reactive gases feeding. The temperatures were controlled by a

multi channel regulator (HORST GmbH, Germany). The ratio of inert gas was set slightly below the ratio in air to obtain the largest amounts of products minimizing the occurrence of strong thermal phenomena.The gases used in Nancy were provided by Messer (purity of 99.95%). Gas flows were controlled by Bronkhorst mass flow controllers.

1.2. Gas chromatography analyses

N-butane analyses were performed using an online gas equipped with a six-gates sampling valve for the introduction of samples taken from the gas at the outlet of the jet-stirred reactor. This gas chromatograph (Agilent 6820) was fitted with a Haysep D packed column and a flame ionization detector. The carrier gas was helium and the oven temperature profile was: 333.15 K during 10 min; ramp at a rate of 5 $K.min^{-1}$ up to 473.15 K; 473.15 K during 62 min. It was used for the quantification of methane, C_2 and C_3 hydrocarbons. The calibration was performed using gaseous standards provided by Air Liquide. The maximum relative uncertainty in the mole fraction was estimated to ±5% with a limit of detection of about 5 ppm

1.3. cw-CRDS cell and analysis

The jet-stirred reactor was coupled to a spectroscopic technique: continuous wave cavity ring-down spectroscopy (cw-CRDS) [5-8]. The cw-CRDS cell consists of a glass tube with an outer diameter of 8 mm and a length of 80 cm. The total volume of the cell including the sampling probe is estimated to be 40 cm^3. The cell is maintained through convection at ambient temperature and the pressure in the CRDS cavity is kept around 10 Torr. The low pressure is obtained using a rotary vane pump (Alcatel 1015SD with a nominal flow rate of 15 $m^3.h^{-1}$).

The cell is connected to the reactor by the mean of a sampling probe. The probe is a fused silica tube with a diameter of 6 mm and a length of about 10 cm. The extremity of the tube, which is located within in the jet-stirred reactor, was thinned by a glass blower to have a very small orifice in order to maintain a low pressure in the cw-CRDS cell (the pressure in the reactor is about 800 Torr). This rapid pressure drop freezes the reaction due to a sharp decrease in concentration and temperature, but also leads to a more selective detection due to reduced pressure broadening of the absorption lines. The flow through this orifice into the CRDS cell is estimated to be 90 $cm^3.min^{-1}$ STP, obtained by measuring the pressure increase in the cw-CRDS cell after closing the pump valve. This flow leads to a residence time of the

gas mixture within the CRDS cell of roughly 0.3 s. The same type of sampling probe has already been used to take samples in flames [9].

CRDS analyses were carried out in the near infrared at wavelengths from 6638 – 6643cm^{-1}. The near-infrared beam was provided by a fibred distributed feed-back (DFB) diode laser (Fitel-Furukawa FOL15DCWB-A81-W1509) emitting up to 40 mW, the wavelength can be varied in the range 6640±13 cm^{-1} through changing the current applied to the diode laser. The diode laser emission is directly fibred and passes through a fibred optical isolator and a fibred acousto-optical modulator (AOM, AA Opto-Electronic). The AOM allows the laser beam to be deviated within 350 ns with respect to a trigger signal for a total duration of 1.5 ms. The zero order beam is connected to a fibred optical wave meter (228 Bristol Instruments) for monitoring the wavelength of the laser emission with an accuracy of 0.01 cm^{-1}. The main first order laser beam is coupled into the CRDS optical cavity through a short focal length lens (f = 10 mm) for mode matching so as to excite the fundamental TEM_{00} mode. Two folding micrometric mirrors allow easy alignment of the beam, as shown in Figure 1 (main text). After many round trips, the optical signal transmitted through the cavity is converted into current by an avalanche photodiode (Perkin Elmer C30662E). A home designed amplifier-threshold circuit converts the current signal to an exploitable voltage signal and triggers the AOM to deviate the laser beam (turn off of the first order) as soon as the cavity comes into resonance and the photodiode signal exceeds a user-defined threshold. The photodiode signal is connected to a fast 16 bit analogue acquisition card (PCI-6259, National Instruments) in a PC, which is triggered also by the amplifier-threshold circuit. The acquisition card has an acquisition frequency of 1.25 MHz and thus the ring-down signal is sampled every 800 ns and the data are transferred to PC in real time. The ring-down time τ is obtained by fitting the exponential decay over a time range of seven lifetimes by a Levenberg-Marquardt exponential fit in LabView. The concentration of a species being formed or consumed during the hydrocarbon oxidation process in a jet-stirred reactor (JSR), can be obtained by measuring the ring-down time of the empty cavity τ_0, i.e., the ring down time before heating the reactor, and the ring down time τ, after turning on the heater:

$$\alpha = [A] \times \sigma = \frac{R_L}{c}\left(\frac{1}{\tau} - \frac{1}{\tau_0}\right) \quad (1)$$

where σ is the absorption cross section, R_L is the ratio between the cavity length L, i.e. the distance between the two cavity mirrors to the length L_A over which the absorber is present

(see section on CH_4 quantification), c is the speed of light. Knowing the absorption cross section σ, one can extract the concentration [A] of the target molecule.

1.4. Inert coating of the wall of the reactor

For some experiments, as shown in figure S3, the walls of the reactor have been fully covered by a inert coating: SilcoNert™ 2000 surface treatment which eliminates surface adsorption of active compounds on steel, glass, ceramic and carbon surfaces and which was provided by SilcoTeck.

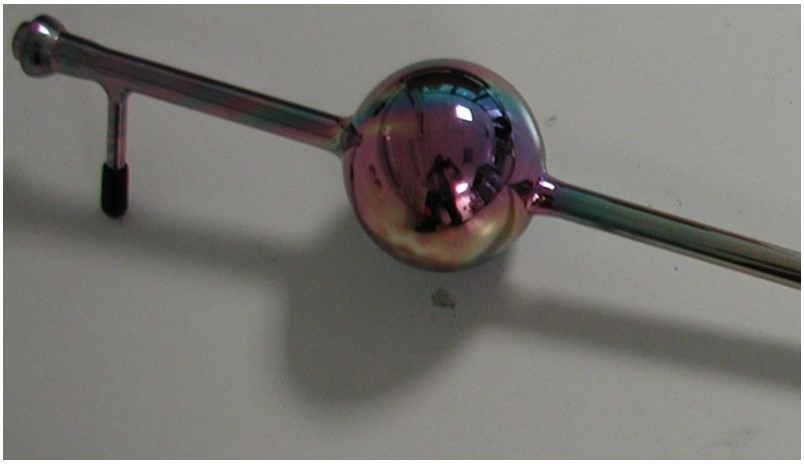

Figure S3. Photography of the treated reactor.

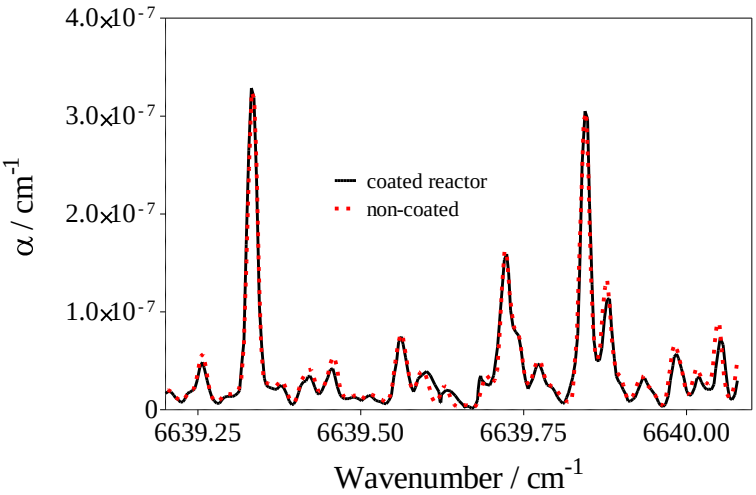

Figure S4. CRDS spectra obtained with reactor walls fully covered by the SilcoNert™ 2000 surface treatment and with reactor walls without any special treatment.

Figure S4 presents CRDS spectra obtained with the walls of the reactor coated by the SilcoNert™ 2000 surface treatment and with walls without any special treatment. It can be observed that no difference is observed between these two spectra.

2. Description of the model used for simulations

The simulations were performed using the software PSR of CHEMKIN [9]. The mechanism of the low-temperature oxidation of n-butane (available on request) has been automatically generated using EXGAS software. This software has already been used for generating mechanisms in the case of a wide range of alkanes [11][12] and alkenes [13]. The reaction mechanisms generated by EXGAS are made of three parts:

- A comprehensive primary mechanism, where the only molecular reactants considered are the initial organic compounds and oxygen. According to the reaction scheme of the oxidation of alkanes described in the main text of this paper, the reactant and the primary radicals are systematically submitted to different types of following elementary steps :
  - Unimolecular initiations involving the breaking of a C-C bond.
  - Bimolecular initiations with oxygen to produce alkyl and $\bullet HO_2$ radicals.
  - Oxidations of alkyl radicals with O_2 to form alkenes and $\bullet HO_2$ radicals.
  - Additions of alkyl (R•) and hydroperoxyalkyl (•QOOH) radicals to an oxygen molecule.
  - Isomerizations of alkyl and peroxy radicals (ROO• and •OOQOOH) involving a cyclic transition state for •OOQOOH radicals.
  - Decompositions of radicals by β-scission involving the breaking of C-C or C-O bonds for all types of radicals (for low temperature modelling, the breaking of C-H bonds is neglected).
  - Decompositions of hydroperoxyalkyl radicals to form cyclic ethers and •OH radicals.
  - Metatheses involving H-abstractions by radicals from the initial reactants.
  - Recombinations of radicals.
  - Disproportionations of peroxyalkyl radicals with $\bullet HO_2$ to produce alkylhydroperoxides and O_2 (disproprtionnations between two peroxyalkyl radicals or beween peroxyalkyl and alkyl radicals are not taken into account).
- A C_0-C_2 reaction base, including all the reactions involving radicals or molecules containing less than three carbon atoms. The fact that no generic rule can be derived for the generation of the reactions involving every compounds containing less than three atoms of carbon makes the use of this reaction base necessary.

- A lumped secondary mechanism, containing the reactions consuming the molecular stable products of the primary mechanism, which do not react in the reaction base. For reducing the number of reactants in the secondary mechanism, the molecules formed in the primary mechanism, with the same molecular formula and the same functional groups, are lumped into one unique species, without distinguishing between the different isomers. The writing of the secondary reaction is made in order to promote the formation of C_{2+} alkyl radicals, the reactions of which are already included in the primary mechanism [12].

Thermochemical data for molecules or radicals were automatically calculated and stored as 14 polynomial coefficients, according to the CHEMKIN II formalism [9]. These data were automatically calculated using software THERGAS [14], based on the group and bond additivity methods proposed by Benson [15].

The kinetic data of isomerisations, recombinations and the unimolecular decompositions are automatically calculated based on the thermochemical kinetics methods [15] using the transition state theory or the modified collision theory. The kinetic data, for which the calculation is not possible by KINGAS [12], are estimated from correlations, which are based on quantitative structure-reactivity relationships and obtained from a literature review [11].

4. Supplementary References

[1] R. Bounaceur, I. Da Costa, R. Fournet, F. Billaud, F. Battin-Leclerc, *Int. J. Chem. Kin.* **2005**, 37, 25-19.

[2] J. Biet, M.H. Hakka, V. Warth, P.A. Glaude, F. Battin-Leclerc, *Energy and Fuel* **2008**, 22, 2258-2269.

[3] M.H. Hakka, P.A. Glaude, O. Herbinet, F. Battin-Leclerc, *Combust. Flame* **2009**, 156, 2129-2144.

[4] D. Matras, J. Villermaux, *Chem. Eng. Sci.* **1973,** 28, 129-137.

[5] C. Bahrini, A. Parker, C. Schoemaecker, C. Fittschen, *Appl. Catal. B-Environ*. **2010**, 99, 413-419.

[6] Z.-W. Liu, Y. Xu, X.-F. Yang, A.-M. Zhu, G.-L. Zhao, W.-G. Wang, *J. Phys. D: Appl. Phys.* **2008**, 41.

[7] M. Djehiche, A. Tomas, C. Fittschen, P. Coddeville, *Z. Phys. Chem.* **2011**, 225, 983-992.

[8] J. Thiébaud, C. Fittschen, *Appl. Phys. B-Lasers Opt*. **2006**, 85, 383-389.

[9] E. Pousse, Z.Y. Tian, P.A. Glaude, R. Fournet, F. Battin-Leclerc, *Combust. Flame* **2010**, 157, 1236-1260.

[10] R.J. Kee, F.M. Rupley, J.A. Miller, *Chemkin II: A fortran chemical kinetics package for the analysis of a gas-phase chemical kinetics*, SAND89-8009B, Sandia Laboratories, **1993**.

[11] F. Buda, R. Bounaceur, V. Warth P.A. Glaude, R. Fournet, F. Battin-Leclerc, *Combust. Flame* **2005**, 142, 170-186.

[12] V. Warth, N. Stef, P.A. Glaude, F. Battin-Leclerc, G. Scacchi, G.M. Côme, *Combust. Flame* **1998**, 114, 81-102.
[13] S. Touchard, R. Fournet, P.A. Glaude, V. Warth, F. Battin-Leclerc, G. Vanhove, M. Ribaucour, R. Minetti., *Proc. Combust. Inst.* **2005**, 30, 1073-1081.
[14] C. Muller, V. Michel, G. Scacchi, G.M. Côme, *J. Chim. Phys.* **1995**, 92, 1154-1178.
[15] S.W. Benson, *Thermochemical Kinetics*, 2nd ed., John Wiley, New York, **1976**.